Biochimica et Biophysica Acta 1840 (2014) 53–64

Contents lists available at ScienceDirect

Biochimica et Biophysica Acta

journal homepage: www.elsevier.com/locate/bbagen

Adaptive responses to glucose restriction enhance cell survival, antioxidant capability, and autophagy of the protozoan parasite *Trichomonas vaginalis*

Kuo-Yang Huang [a,b], Yi-Ywan Margaret Chen [d], Yi-Kai Fang [a,b], Wei-Hung Cheng [a,b], Chih-Chieh Cheng [a], Yu-Chuen Chen [b], Tiffany E. Wu [b], Fu-Man Ku [b], Shih-Chieh Chen [b], Rose Lin [b], Petrus Tang [b,c,*]

[a] *Graduate Institute of Biomedical Sciences, College of Medicine, Chang Gung University, Kwei-Shan, Taoyuan 333, Taiwan*
[b] *Molecular Regulation and Bioinformatics Laboratory, Department of Parasitology, College of Medicine, Chang Gung University, Kwei-Shan, Taoyuan 333, Taiwan*
[c] *Bioinformatics Center, Chang Gung University, Kwei-Shan, Taoyuan 333, Taiwan*
[d] *Department of Microbiology and Immunology, College of Medicine, Chang Gung University, Kwei-Shan, Taoyuan 333, Taiwan*

ARTICLE INFO

Article history:
Received 7 May 2013
Received in revised form 22 July 2013
Accepted 13 August 2013
Available online 17 August 2013

Keywords:
T. vaginalis
Glucose restriction
RNA sequencing
Glutamate dehydrogenase
Autophagy

ABSTRACT

Background: To establish an infection in the vagina, *Trichomonas vaginalis* must adapt to various environmental cues for survival and further replication. Nutrient competition by lactobacilli, the major normal vaginal flora, is one of the mechanisms to limit the growth of other microorganisms. Additionally, lactobacilli produce H_2O_2 that can reduce the genital infections caused by other pathogens. Thus, the ability to overcome the metabolic stresses, such as glucose restriction (GR), as well as the oxidative stresses, is critical for *T. vaginalis* to establish an infection.
Methods: To gain insights into the molecular mechanisms of adaptation to GR, we utilized next-generation RNA sequencing (RNA-seq) to quantify the gene expression changes upon GR. Autophagy, a cytoprotective response to starvation, was monitored by using autophagy-specific staining, autophagy inhibition assay, and co-localization of autophagosomes with lysosomes.
Results: We demonstrated that GR promotes the survival of *T. vaginalis*. Besides, GR-cultivated cells exhibit higher H_2O_2 resistance. Our RNA-seq data revealed that genes involved in general energy metabolism were downregulated, whereas genes encoding glutamate metabolism-related aminotransferases were strikingly upregulated under GR. Furthermore, autophagy was first identified and characterized in *T. vaginalis* under GR.
Conclusions: These data suggest that GR induces a metabolic reprogramming, enhancing antioxidant ability and autophagy for cellular homeostasis to maintain survival.
General significance: Our work not only led to significant advances in understanding the transcriptional changes in response to GR but also provided possible strategies elicited by GR for *T. vaginalis* to adapt to the vaginal microenvironment.

1. Introduction

Nutrient sensing and responses to starvation are tightly regulated for energetic homeostasis and cell survival. Since glucose is the foremost energy source in the majority of eukaryotic cells, many studies have investigated the effects of glucose restriction (GR) on metabolism, stress responses, regulation of cell survival and cell death, to understand the adaptive mechanisms under nutritional stresses [1,2]. Previous studies reported that decreased glucose availability in the unicellular model *Saccharomyces cerevisiae* results in several physiological changes, including a metabolic shift from fermentation to respiration [3], translational suppression [4], enhanced resistance to oxidative stress [5] and autophagy [6]. However, the mechanisms by which nutritional stresses trigger adaptive signaling remain poorly understood in protists.

Trichomoniasis is the most common nonviral sexually transmitted infection (STI) caused by the parasitic protozoan *Trichomonas vaginalis*, with more than 170 million cases annually worldwide. Trichomoniasis leads to serious health outcomes for women, including vaginitis, preterm delivery, infertility, low birth weight infants, susceptibility to HPV, herpes virus and cervical cancer [7]. In males, *T. vaginalis* infection is usually

Abbreviations: GR, glucose restriction; CR, caloric restriction; NGS, next generation sequencing; RNA-seq, RNA sequencing; GK, Glucokinase; GPI, Glucose phosphate isomerase; PFK, Phosphofructokinase; ALDO, Fructose-1,6-bisP aldolase; TPI, Triose-phosphate isomerase; GAPDH, Glyceraldehyde 3-P dehydrogenase; PGK, Phosphoglycerate kinase; PGAM, phosphoglycerate mutase; ENO, Enolase; PEPCK, Phosphoenolpyruvate carboxykinase; MDH, Malate dehydrogenase; PK, Pyruvate kinase; ME, Malic enzyme; ALT, Alanine aminotransferase; ADH, Alcohol dehydrogenase; LDH, Lactate dehydrogenase; GDH, Glutamate dehydrogenase; SOD, Superoxide dismutase; TrxP, Thioredoxin peroxidase; Rbr, rubrerythrin; ROS, reactive oxygen species

* Corresponding author at: Molecular Regulation and Bioinformatics Laboratory, Department of Parasitology, 259 Wenhwa 1st. Road, Kweishan, Taoyuan 333, Taiwan. Tel.: +886 3 2118800x5136; fax: +886 3 2118122.
E-mail address: petang@mail.cgu.edu.tw (P. Tang).

0304-4165/$ – see front matter © 2013 Elsevier B.V. All rights reserved.
http://dx.doi.org/10.1016/j.bbagen.2013.08.008

asymptomatic, although urethritis and chronic prostatitis are observed in some cases [8]. It has been reported that *T. vaginalis* infection is correlated with increased risk of human immunodeficiency virus transmission [9] and, more recently, lethal prostate cancer [10].

The main energy source for *T. vaginalis* comes from fermentative carbohydrate metabolism under both anaerobic and aerobic conditions [11]. Within the cytoplasm, glucose is converted to pyruvate that is subsequently metabolized by fermentative oxidation in the hydrogenosome. Hydrogenosome, a double membrane organelle analogous to mitochondria, generates ATP through substrate-level phosphorylation [12]. GR is a metabolic stress that has been studied in other protists and, in some cases, is associated with pathogenesis. For instance, PfEMP (*var*) genes, key molecules in malaria pathogenesis, are upregulated upon GR [13]. Additionally, GR induces the differentiation of trophozoites into cysts in *Entamoeba invadens* [14] and boosts *Entamoeba histolytica* virulence [15,16]. *T. vaginalis* is routinely cultivated in medium [17] containing high glucose levels (~58 mM), which is around 10-fold than that of blood. However, it is unlikely that the parasite exposes to such a high concentration of glucose in its natural environment. Hence, it prompts us to uncover the adaptive mechanisms of *T. vaginalis* under GR, shedding light on potential strategies of this parasite to cope with the nutrient stress and establish an infection.

Autophagy, a lysosome-mediated catabolic process for digesting the cytoplasmic constituents, is also widely regarded to be crucial for cell survival under nutritional stresses. Recent studies suggest that autophagy correlates with the pathogenicity of several protists [18]. For example, autophagy is essential for differentiation and virulence in *Leishmania major* [19] and participates in nutritional stress response and differentiation in *Trypanosoma cruzi* [20]. Autophagy also plays a key role in the proliferation and differentiation of the enteric protozoan *Entamoeba* [21]. More recently, it has been shown that the self-digestion process is associated with cell death under nutrient-limited condition in *Blastocystis* [22], *Trypanosoma brucei* [23] and *Toxoplasma gondii* [24]. Given the importance of autophagy in these protists and the lack of information on this process in trichomonads, we aim to unravel the molecular mechanisms of autophagy under GR.

Recently, high-throughput next generation sequencing (NGS) approaches have dramatically improved the efficiency of gene discovery, allowing for the detection of transcripts with very low abundance [25]. The reliable technique provides a great opportunity to dissect the heavily duplicated genome of *T. vaginalis*. To better understand the molecular mechanisms involved in the adaptive responses to GR, we performed NGS-based RNA sequencing (RNA-seq) to profile genome-wide mRNA changes prompted by GR. We highlighted the most differentially regulated genes responsible for the major energy-producing and oxidative stress-related pathways, hopefully providing insights into the molecular components required for adaptation to the metabolic stress and the mechanisms for establishment of an infection.

2. Materials and methods

2.1. T. vaginalis culture conditions

The *T. vaginalis* ATCC30236 trophozoites were maintained in YIS medium [17], pH 5.8, containing 10% heat-inactivated horse serum and 1% glucose at 37 °C. For GR experiments, the trophozoites were grown in the same medium without glucose supplement [16]. Recovery assay was done by adding 1% glucose to the GR-cultivated parasites. Growth of the parasites was monitored by using trypan blue exclusion hemocytometer counts.

2.2. Determination of extracellular glucose concentration

The concentration of glucose in glucose-rich (with 1% glucose) and GR medium was measured by the glucose assay kit (Biovision) according to the manufacturer's instructions. Medium (2 μl/assay) from the glucose-rich and GR cultivation was diluted in Glucose Assay Buffer. The reaction mixture (46 μl Glucose Assay Buffer, 2 μl Glucose Probe and 2 μl Glucose Enzyme Mix) was added to glucose standard and test samples. The reaction was incubated for 30 min at 37 °C in the dark. Glucose enzyme mix specifically oxidizes glucose to generate a product which reacts with a dye to generate color ($\lambda = 570$ nm). The concentration was determined by measuring the O.D. value 570 nm using the spectrophotometer.

2.3. Glutamate dehydrogenase (GDH) activity assay

GDH activity was determined by the GDH activity assay kit (Biovision) according to the manufacturer's instructions. Briefly, 10 μl of NADH stock solution (10 mM) was diluted with 90 μl of GDH assay buffer, which is used to plot the NADH standard curve by adding 0, 2, 4, 6, 8, and 10 μl into a 96-well plate. The final volume was adjusted to 50 μl with GDH assay buffer. Trophozoites (1×10^6 cells) of test samples were harvested and homogenized in 200 μl ice-cold assay buffer. 10 μl of samples was diluted with assay buffer to the final volume of 50 μl. 100 μl reaction mixtures (82 μl assay buffer, 8 μl GDH developer, and 10 μl glutamate) were added to each well containing the test samples and standards. The reaction was incubated for 10 min at 37 °C and the GDH activity was determined by measuring the O.D. at 450 nm. The final GDH activity (nmol/min/ml) was calculated by the equation $B/T \times V$: B is the NADH amount (nmol). T is the incubation time (min). V is the sample volume (ml).

2.4. Hydrogen peroxide survival assay

Cells grown in glucose-rich or GR medium containing 10% heat-inactivated horse serum for 24 h at 37 °C were treated with 0, 0.5 mM, and 1 mM freshly-prepared H_2O_2 (MERCK) for 2 h. The initial cell density of these conditions was ~1×10^6 cells/ml. The number of viable cells was determined every 30 min by trypan blue exclusion using a hemocytometer.

2.5. RNA extraction, cDNA synthesis and quantitative PCR (qPCR)

Total RNA was extracted by using the TRI Reagent® (Molecular Research Center) from GR cultures of various incubation time (12 h, 24 h, 36 h) and cells grown in glucose-rich condition at mid-log phase (1%_12 h). Reverse transcription (RT) was carried out in a reaction mixture containing 5 μg total RNA, 50 nM RT primer, 0.25 mM dNTPs, 0.75 U/μl ThermoScript™III reverse transcriptase, 0.2 U/μl RNase out, and 0.05 M DTT (ThermoScript™III RT-PCR System, Invitrogen). The RT reaction mixture was incubated at 65 °C for 5 min, 50 °C for 60 min and then stopped at 70 °C for 15 min. qPCR was performed as previously described [26]. Briefly, the 20 μl PCR mixtures contain 1 μg reverse transcription product, master mix (Ampliqon), 0.5 μM forward and reverse primers. Primer pairs used in this study were listed in Table S6.

2.6. Library preparation for RNA-seq

Total RNA from cells cultivated under GR at 12 h, 24 h, 36 h and cells grown in 1% glucose at mid-log phase (1%_12 h) were isolated as mentioned above and stored at −80 °C. Approximately 10 μg of total RNA was sent to Beijing Genomics Institute (BGI) for mRNA purification and cDNA library construction as previously described [27]. High-throughput RNA-seq was conducted on the next-generation sequencer HiSeq™ 2000 (Illumina) using the HiSeq Flow Cell v3, TruSeq™ PE Cluster Kit v3 Reagent for cluster generation, and TruSeq™ SBS Kit v3 for sequencing by synthesis.

2.7. RNA-seq data analysis

Reference transcript sequences and their annotation were downloaded from TrichDB V1.3 [28]. Paired-end gene reads were imported and mapped to the *T. vaginalis* G3 annotated reference

Table 1
Summary of RNA-seq mapping statistics.

Group[a]	Reads generated	Mapped reads	% of mapped reads	Average read length (base)	Total bases
1%_12 h	51,519,438	49,705,292	96.48	89.46	4,608,943,825
GR_12 h	27,374,828	24,728,822	90.33	86.72	2,373,884,281
GR_24 h	26,119,804	22,697,719	86.90	87.21	2,278,033,053
GR_36 h	26,110,496	21,830,466	83.61	87.55	2,285,868,362

[a] These cDNA libraries were constructed from cells cultivated under 1% glucose at mid-log phase (1%_12 h) and GR with different incubation time (GR_12 h, GR_24 h,GR_36 h).

transcripts using CLC Genomics Workbench software (Version 5.0.1). The following mapping parameters were used: length fraction = 0.9, similarity = 0.8, minimum distance = 120 and maximum distance = 300. The mapping reports were exported and summarized in Table 1. The expression of each gene was normalized as values corresponding to the number of reads per kilobase per million mapped reads (RPKM). This strategy makes it possible to use RPKM values for differential gene expression analysis between RNA-seq datasets since the length of the reference contig is the same. RPKM values of 32147 expressed genes from glucose-rich and GR RNA-seq datasets were listed (File S1). Differential gene expression changes were represented as $\log_2$ fold changes (RPKM of genes at the log phase of GR compared with that of glucose-rich cultivation and RPKM of genes at different time intervals of GR compared with GR_12 h). Heatmaps showing the expression patterns were generated by using MultiExperiment Viewer (Mev).

2.8. Genome-wide survey of autophagy-related (Atg) genes in T. vaginalis

Atg protein sequences in yeast, mice, and human were retrieved from the Autophagy Database [29] and served as queries to search for Atg orthologues in *T. vaginalis* (Table S4) using the local blast algorithm [30] against *T. vaginalis* protein sequences downloaded from TrichDB [28]. The E-values of hits lower than 10^{-10} were considered significant and further submitted for conserved domain searches to verify the Atg functional motifs using the NCBI conserved domain searched engine [31].

2.9. Autophaghy detection

To test for the presence of autophagy in *T. vaginalis*, cells cultivated under GR and glucose-rich medium containing 10% heat-inactivated horse serum were stained with Cyto-ID™ green fluorescent dye (Enzol) for the detection of autophagic vacuoles as previously described [32,33]. Approximately 2×10^5 cells cultivated under GR from different time intervals (12 h, 24 h, 36 h) and 1% glucose at mid-log phase were harvested. The pellet was resuspended in 100 μl Dual Detection Reagent (1 ml of 1× Assay Buffer containing 2 μl of Cyto-ID™ Green Detection Reagent and 2 μl of Hoechst 33342 nuclear stain) and incubated for 30 min at 37 °C. Fluorescent images were obtained by using a fluorescent microscope (Zeiss). Standard GFP, RFP, and DAPI filter sets were used for imaging the autophagic, lysosomal and nuclei signals, respectively. For autophagy inhibition assay, GR-cultured cells (GR_24 h and GR_36 h) were treated with 50 μM wortmannin (Invivogen) for 6 h at 37 °C, followed by autophagy detection as mentioned above. To evaluate the inhibitory effect of wortmannin on autophagy, the average number of autophagic vesicles per cell was determined by counting the fluorescent punctate in cells [34] after treatment with wortmannin compared with the untreated group. A total of 80 cells (40 cells per group) were examined for each condition.

2.10. Autophagy quantization

Approximately 2×10^5 cells were harvested and the pellet was resuspended in 0.5 ml of freshly diluted Cyto-ID™ Green Detection Reagent (4 ml of 1× Assay Buffer containing 1 μl of Cyto-ID™ Green Detection Reagent). Samples were incubated for 30 min at 37 °C and the autophagic signal was immediately analyzed and quantified by using a FASCan flow cytometer (BD Biosciences).

2.11. Confocal microscopy examination of Cyto-ID™ and Lysotracker Red costaining

For detection of co-localization of autophagosomes with lysosomes, approximately 3×10^5 cells were harvested and costained with Cyto-ID ™ (1 ml of 1× Assay Buffer containing 2 μl of Cyto-ID™ Green Detection Reagent, 100 μl/sample) and 100 nM Lysotracker Red DND-99 (Invitrogen) for 30 min at 37 °C. After incubation, 10 μl of the cell suspension was applied to POC-R chamber (Zeiss) and overlay with a coverslip. Fluorescent images were obtained using a confocal microscope (Zeiss LSM510). Excitation and emission spectra for Cyto-ID™ green dye and Lysotracker Red were 463/534 nm and 577/590 nm, respectively. Quantitation of co-localized fluorescent signals in cells (n = 11) was presented as the Pearson's correlation coefficient [35] analyzed by LSM image examiner software.

3. Results and discussion

3.1. GR promotes cell survival in T. vaginalis

We previously demonstrated that carbohydrate metabolism-related genes and proteins represent the most abundant group in the transcriptome and proteome of trophozoites grown in the standard culture medium containing 1% glucose [36], indicating that glycolysis is one of the most critical processes for *T. vaginalis* under glucose-rich condition. A previous study showed that the median level of glucose in vaginal secretions of healthy women was approximately 5 mM [37]. However, the exact glucose acquisition for *T. vaginalis* also remains unknown. Compared to glucose concentration in vagina secretions (~0.1%), 1% glucose appears to be more than needed for *T. vaginalis* to establish an infection in the vagina. Furthermore, vaginal lactobacilli limit the growth of other microorganisms by competition for glucose [38]. Hence, the adaptation to glucose deprivation is likely a critical strategy for *T. vaginalis* to establish an infection. To verify the effect of glucose on the survival of *T. vaginalis*, we monitored the viability of cells cultivated in medium with 1% glucose (glucose-rich; initial glucose concentration 58.196 mM) and without additional glucose (GR). Since serum contains small amounts of blood glucose, the initial glucose concentration in GR medium was estimated to be 0.352 mM (Fig. S1A). The number of viable cells in the glucose-rich group reached stationary phase at 24 h with a cell density of 4×10^6 (cells/ml), followed by a rapid decline (Fig. 1A). Almost all cells were dead at 42 h under glucose-rich cultivation. On the other hand, *T. vaginalis* maintained a constant survival rate under GR cultivation, with a cell density of ~2×10^6 (cells/ml) from 24 h to 48 h (Fig. 1A), and a cell density of ~5×10^5 (cells/ml) at 108 h. The proportion of dead cells reached ~80% at 36 h under glucose-rich cultivation, whereas it was less than 20% at 36 h and reached ~80% at 72 h under GR (Fig. 1B). The glucose concentration remained greater than 30 mM in glucose-rich medium after 24 h cultivation, whereas it was less than 0.1 mM in GR medium after 12 h (Fig. S1A), implying that the parasite utilizes alternative energy sources to maintain growth and survival during GR.

To confirm that the prolonged survival was indeed GR-dependent, we monitored the viability of GR-cultured cells (mid-log phase) supplemented with 1% glucose (Fig. 1C). The data indicated that glucose was a preferential source for cell division, reaching a peak cell density of ~4×10^6 (cells/ml) at 24 h in the glucose-treated group, but followed by a rapid cell death, again supporting the hypothesis that GR promotes survival. To test whether cells grown under GR were still physiologically active, we transferred GR cultures at different time intervals to fresh standard culture medium and determined the cell division times (Fig. 1D).

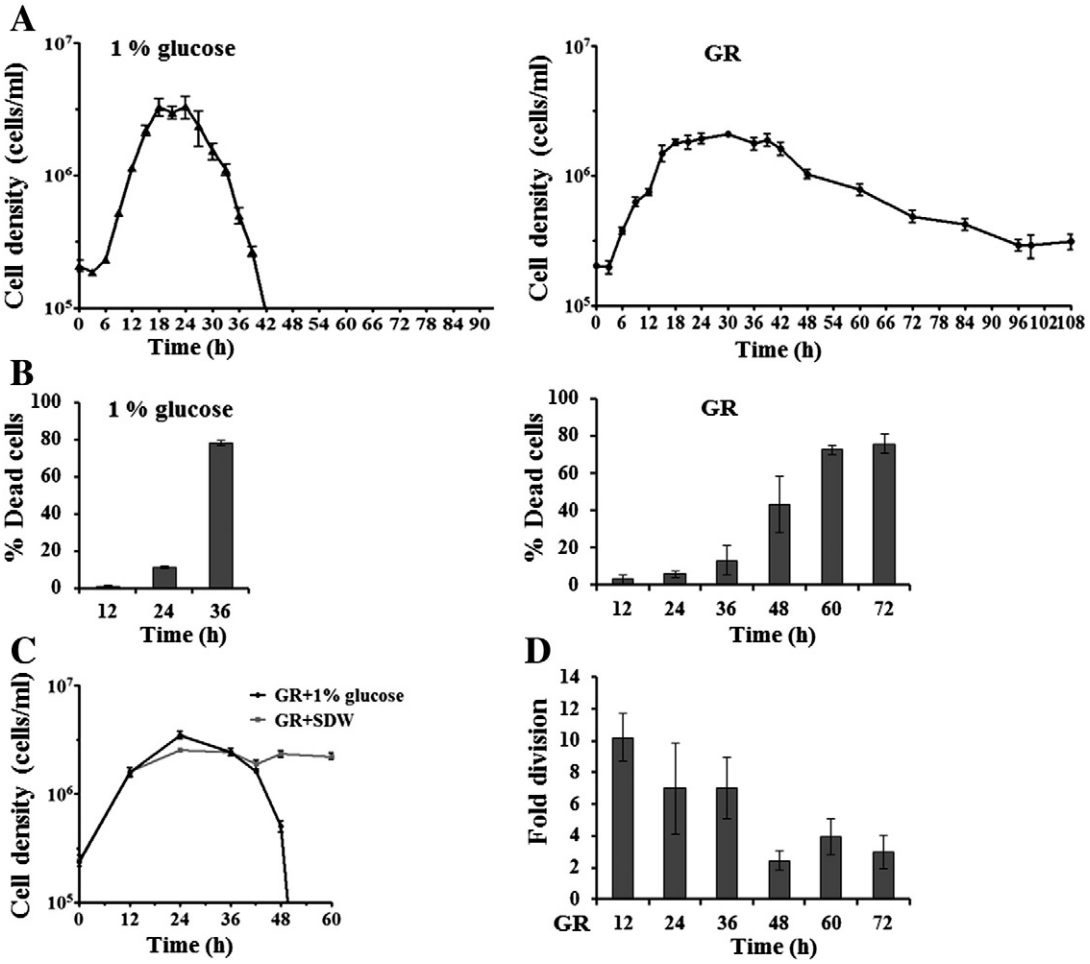

Fig. 1. Glucose restriction (GR) promotes survival of *T. vaginalis*. (A) The effect of GR on the growth of *T. vaginalis* was examined. The initial concentration of trophozoites cultivated in YIS medium with 1% glucose (glucose-rich) and without additional glucose (GR) was ~2 × 10^5/ml. The cell density of each group was monitored by using trypan blue exclusion hemocytometer counts. (B) The ratio of dead cells under glucose-rich and GR cultivation was determined. (C) The effect of glucose supplement on the survival of GR-cultivated cells. The viability of GR-cultivated cells (mid-log phase) treated with 1% glucose (black line) and the same volume of sterile distilled water (gray line) was monitored. (D) Determination of the division ability of GR-cultured cells when cultivated in glucose-rich medium. 1 ml cells from GR cultivation at different time intervals (12 h, 24 h, 36 h, 48 h, 60 h) were transferred to 9 ml fresh glucose-rich medium and the fold increase of cells was monitored after 12 h incubation. All data (A to D) represented the means ± SD of three independent experiments.

The result indicated that cells cultivated under GR before 36 h have good division ability with the cell number increasing 6 times within 12 h in glucose-rich medium, whereas cells grown under GR after 48 h only can increase 2–4 times.

Dietary restriction has been shown to increase lifespan in organisms ranging from yeast to mammals [39]. Previous studies in *S. cerevisiae* indicated that acidic metabolites produced under glucose-rich cultivation are a primary factor leading to apoptosis-like response and limit the lifespan of yeast cells [40]. To verify whether the mechanism also occurs in *T. vaginalis*, we measured the pH during glucose-rich and GR cultivation (Fig. S1B). Of note, the pH of glucose-rich cultivation is ~4.6 at 24 h, reducing to ~4.2 at 36 h, whereas the pH is maintained at ~5.5 during GR cultivation. The products through GR metabolism appeared to be not so acidic and thereby *T. vaginalis* could maintain survival. Indeed, the vaginal acidic pH maintained by *Lactobacillus* has been shown to inhibit the growth of *T. vaginalis* [41]. Although GR enhances virulence in *Entamoeba* [15,16] and *Plasmodium* [13], the survival of these protists in response to GR seems to be unaffected. We provided the first evidence that GR induces a longevity-like phenomenon among the protists. Further investigations of the mechanistic details underlying the phenomenon are likely to reveal new perspectives on the pathogenesis of this pathogen.

3.2. Extensive transcriptome profiling of T. vaginalis in response to GR by RNA-seq

Previous analyses of large-scale gene expression in *T. vaginalis* at different conditions, such as various iron supplement [42] and fibronectin-induced amoeboid transformation [36], have been carried out mainly by Expressed sequenced tags (EST) sequencing. These transcriptomic studies provided useful data for interrogating the biology of *T. vaginalis* in response to different environmental cues; however, more in-depth and extensive analyses are required to dissect the regulation of massively duplicated gene families in the *T. vaginalis* genome. To better understand the transcriptional changes modulating the adaptation during glucose deprivation, we conducted RNA-seq analyses of *T. vaginalis* under GR (12 h, 24 h, 36 h) and glucose-rich cultivation (1% glucose at 12 h) to obtain dynamic gene expression profiles. A total of 51,519,438 and 79,605,128 raw sequencing reads were generated from the glucose-rich and 3 GR cDNA libraries, respectively (Table 1). Of these reads, 49,705,292 (96.48%) and 69,257,007 (with an average of 86.95%) from the glucose-rich and GR datasets were matched to the genome of *T. vaginalis*, giving rise to 4,608,943,825 and 6,937,785,696 bases, respectively. The reads mapped to a total of 32,147 protein-coding genes in glucose-rich and GR conditions (File S1). We observed a trend that

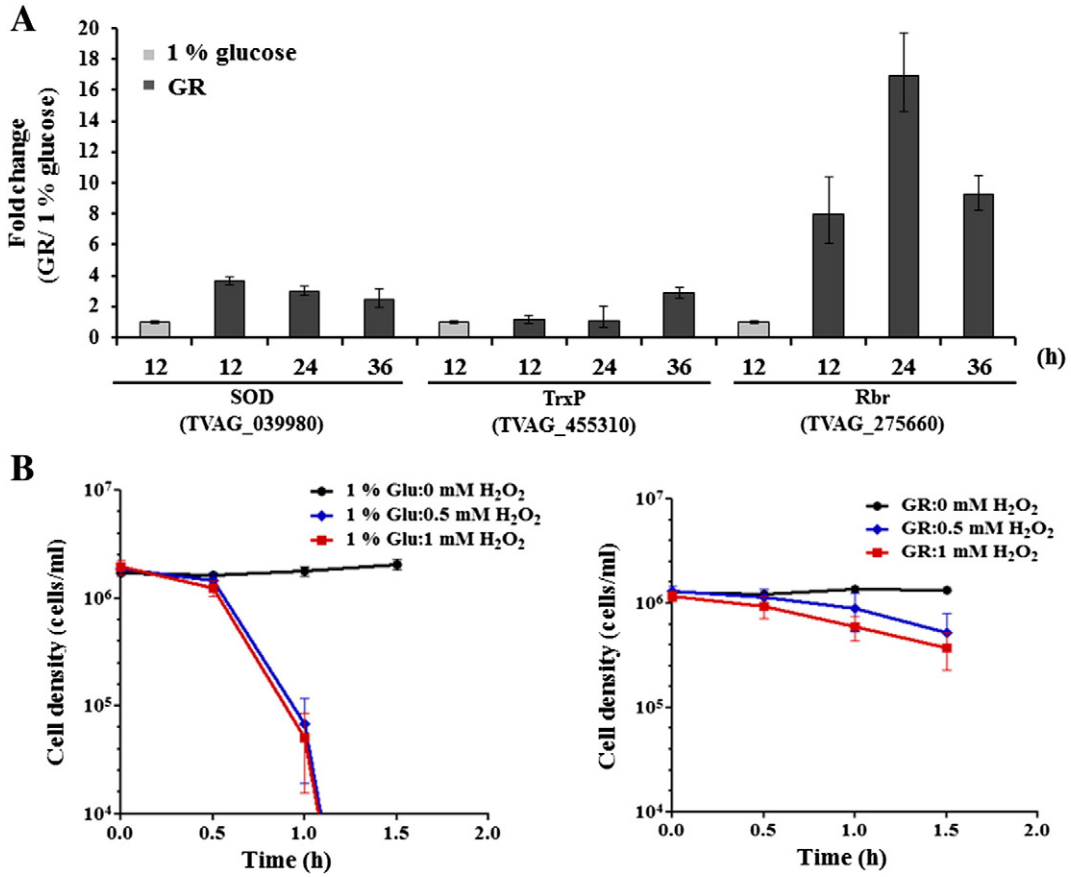

Fig. 2. GR induces antioxidant gene expression and enhances H_2O_2 resistance in *T. vaginalis*. (A) The genes encoding superoxide dismutase (SOD), thioredoxin peroxidase (TrxP), and rubrerythrin (Rbr) with significant upregulation upon GR determined by RNA-seq was validated by qPCR. The quantitative expression data was represented as fold induction (GR_12 h-GR_36 h/1%_glucose 12 h) ± SD of the means of three independent experiments. (B) Determination of the antioxidant ability of cells cultivated under GR compared with glucose-rich condition. Cells grown under 1% glucose and GR conditions at late log phase (~24 h) were adjusted to the same cell density (~1 × 10^6 cells/ml) and followed by treatment with 0, 0.5 and 1 mM H_2O_2. The number of viable cells was monitored every 30 min by trypan blue exclusion using a hemocytometer. Data represented the means ± SD of three independent experiments.

several gene copies within a gene family were expressed at very low levels (RPKM < 10). Although massive paralogue retention has been considered a unique feature of the *T. vaginalis* genome [42], the underlying mechanism remained yet unknown. To validate the RNA-seq data, we determined the expression levels of 10 upregulated (superoxide dismutase, SOD, TVAG_039980; thioredoxin peroxidase TrxP, TVAG_455310; rubrerythrin, Rbr, TVAG_275660; major facilitator superfamily, MFS, TVAG_193600, TVAG_565650, TVAG_345280; glutamate dehydrogenase, GDH, TVAG_072100, TVAG_025910, TVAG_201620; alanine dehydrogenase, AlaDH, TVAG_235800) and 2 downregulated genes (malate dehydrogenase, MDH, TVAG_171090; pyruvate kinase, PK, TVAG_373720) upon GR by qPCR (Figs. 2A and S2). qRCR analysis confirmed the expression patterns of these transcripts as observed in our RNA-seq data. We provided 4 RNA-seq datasets, with hope to examine effectively the intriguing and sophisticated biology of this parasite during GR. Metabolic reprogramming is the most important adaptation under nutrient deprivation in *E. histolytica* and *Plasmodium falciparum* [16,43]. Also, GR has been shown to extend lifespan by modulation of the oxidative stress response in yeast [44] and *Caenorhabditis elegans* [45,46]. Hence, we mainly focused on the expression changes in the major energy metabolic pathways and antioxidant system in *T. vaginalis*, leading to advances in understanding the adaptive mechanisms of the parasite to survive under the nutritional stress.

3.3. GR modulates oxygen scavenging system

3.3.1. GR induces gene expression responsible for antioxidant ability

Survival extension induced by GR in *S. cerevisiae* is correlated with increased superoxide dismutase (SOD) expression and H_2O_2 levels [44]. To determine whether GR plays a role in the regulation of antioxidant genes in this parasite, we analyzed the expression changes prompted by GR of all the putative antioxidant-related genes identified in the genome [47] (Table S1), some of which have been proved to express in the hydrogenosome [48]. We noted that 5 of 6 SOD gene copies were upregulated at the log and early stationary phases of GR cultivation (total RPKM of 6 gene copies for glucose-rich, GR_12 h and GR_24 h were 5139, 6594, and 8722, respectively) (Table S1). The *T. vaginalis* hydrogenosme contains a thioredoxin-linked peroxiredoxin antioxidant system [49] to remove the detrimental effects of reactive oxygen species (ROS). Thioredoxin peroxidase (TrxP) and rubrerythrin (Rbr) are the enzymes that exert the same function to convert H_2O_2 to H_2O in the hydrogenosome. Intriguingly, Rbr paralogues with RPKM > 10 were strikingly upregulated upon GR (total RPKM for glucose-rich and GR_12 h and GR_24 h were 246, 1482, and 1518, respectively), whereas TrxP paralogues were only slightly upregulated at the early stage of GR (Table S1 and File S1). Activation of SOD and TrxP was observed in *T. vaginalis* exposed to different individual stimuli, such as iron deficiency [42] or adherence to fibronectin [36]. However, there does not appear to be a significant regulation of Rbr in these stress-related conditions, suggesting the potentially important role of Rbr in GR. We selected these antioxidant genes with significant upregulation upon GR for validation by qPCR analysis, which is inconsistent with our RNA-seq data (Fig. 2A). It is tempting to speculate whether upregulation of these antioxidant genes plays a pro-survival role in *T. vaginalis* during the nutritional stress, as proposed in other model organisms [45,46].

3.3.2. GR enhances H_2O_2 resistance in T. vaginalis

To verify whether GR enhances antioxidant ability in *T. vaginalis*, we examined the effect of H_2O_2 on the survival of cells under GR compared with glucose-rich cultivation (Fig. 2B). Cells grown in glucose-rich and GR medium for 24 h were challenged with different amounts of H_2O_2 (0, 0.5 mM, 1 mM) and the cell viability was monitored. Noticeably, GR-cultivated cells were highly tolerant to killing by H_2O_2, maintaining a cell density of ~5×10^5 (cells/ml) after treatment with 1 mM H_2O_2 for 1.5 h. In contrast, almost all cells cultivated under glucose-rich condition were dead after treatment with 0.5 mM H_2O_2 for 1.5 h (Fig. 2B). A general concept of GR is that decreased glucose uptake would lead to a reduction of metabolic rate, thus promoting the cell survival due to less ROS production. However, more recent investigations indicated that ROS formation by GR may trigger cellular signaling resulting in metabolic health and longevity [50–52]. These beneficial effects elicited by mild-level stresses, which is so-called hormesis, have been considered to increase stress resistance and lifespan. Herein, we demonstrated that GR enhances antioxidant capability, which is a hormesis-like phenomenon first identified in *T. vaginalis*.

The toxic and inhibitory effect of H_2O_2-producing lactobacilli against the overgrowth of other pathogens in the vagina was demonstrated [53,54]. Therefore, *T. vaginalis* must have the ability to overcome the oxidative stress and maintain infection. Our data suggested that *T. vaginalis* increases the expression of antioxidant genes in response to GR, which potentially enhances the resistance to H_2O_2, implying a possible survival strategy of *T. vaginalis* against H_2O_2 generated in the vaginal ecosystem.

3.4. Metabolic signatures of T. vaginalis under GR

3.4.1. Central energy metabolism

The transcriptomic profiles of genes encoding glycolytic enzymes under GR and glucose-rich cultivation were shown (Fig. 3 and Table S2). Obviously, many glycolytic enzymes were negatively regulated in the mid-log growth phase of GR cultivation (GR_12 h) compared with that of glucose-rich condition (1% glucose_12 h). Among the top 20 highly expressed genes in the glucose-rich group, 9 of which were carbohydrate metabolic enzymes (File S1). However, once grown under glucose deprivation condition, *T. vaginalis* drastically reduced the expression of these genes. For example, 4 of 5 enolase gene copies with RPKM > 100 under glucose-rich condition were downregulated upon GR (total RPKM of 9 gene copies were 12,624 and 3956 for glucose-rich and GR_12 h, respectively), whereas the other 4 paralogues were expressed at very low levels (RPKM < 10) in all conditions. Similarly, 7 of 8 glyceraldehyde 3-P dehydrogenase (GAPDH) gene copies with RPKM > 100 under glucose-rich condition were downregulated upon GR (total RPKM were 23,816 and 7924 for glucose-rich and GR_12 h, respectively). Other glycolytic gene families, such as fructose-bisphosphate aldolase (ALDO), Triose-phosphate isomerase (TPI), phosphoenolpyruvate carboxykinase (PEPCK), and pyruvate kinase (PK) also exhibited similar expression patterns that were negatively regulated at the log phase of GR (Fig. 3B and Table S2).

Even though we observed a remarkable downregulation of many gene families involved in the glycolytic pathway, a small portion of paralogous copies, such as ALDO (TVAG_345360), phosphoglycerate mutase (PGAM) (TVAG_113710), enolase (TVAG_043500), and phosphofructokinase (PFK) (TVAG_281070), were found to be distinctly upregulated upon GR (Fig. 3B and Table S2). The regulation of the differentially expressed paralogues in response to various nutritional stimuli was also identified by a previous comparative transcriptomic study of *T. vaginalis* [42] under iron-rich and iron-restricted conditions, indicating that one of the four iron-responsive GAPDH paralogues displayed an opposite expression pattern to the other paralogues. It is tempting to speculate whether these paralogues may have specialized functions, as proposed by the previous reports that some metabolic enzymes, such as enolase and GAPDH, have been implicated as adhesion proteins in *T. vaginalis* [55,56].

Recently, the *T. vaginalis* hydrogenosome proteome was established and over 500 proteins were identified [48]. To determine the role of this energy-producing organelle in response to GR, we analyzed the

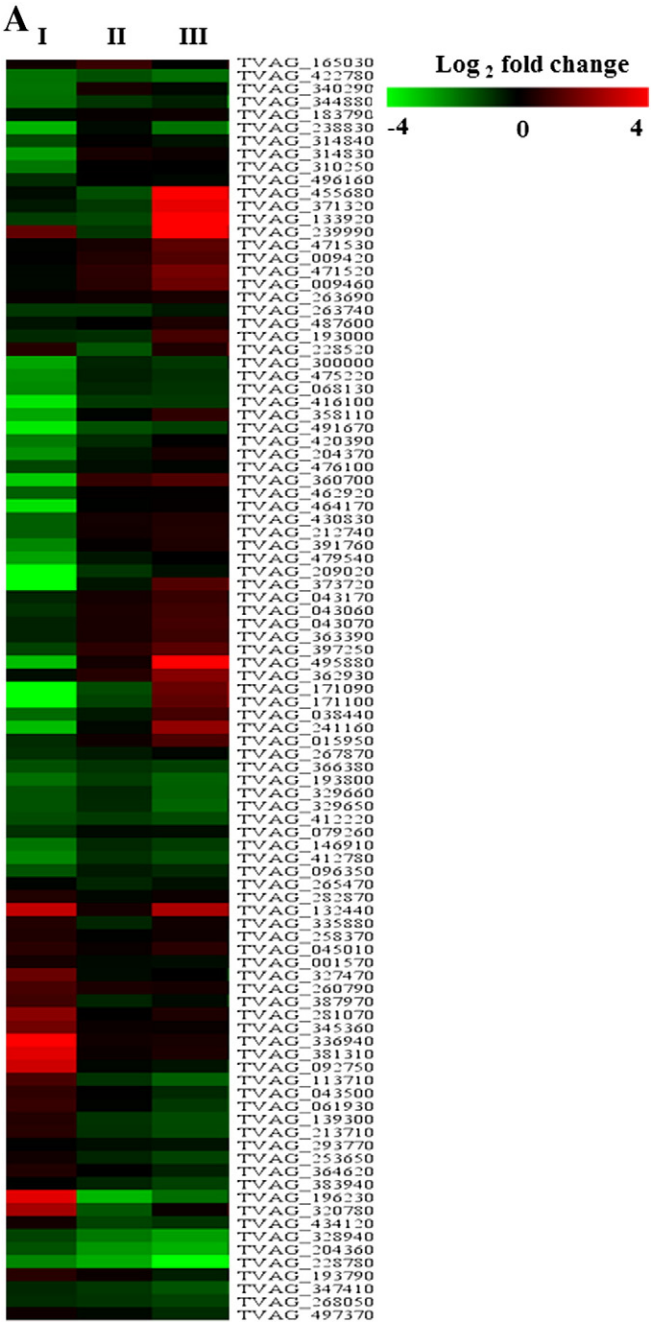

Fig. 3. The effects of GR on differential expression of genes encoding enzymes involved in central energy metabolism in *T. vaginalis*. (A) Heatmap visualization of differentially expressed genes in the glycolytic pathway under GR compared with glucose-rich cultivation. The gene expression changes were represented as $\log_2$ fold changes (RPKM of genes at the log phase of GR compared with that of glucose-rich cultivation. I: GR_12 h/1%_12 h, and RPKM of genes at different time intervals of GR compared with GR_12 h, II: GR_24 h/GR_12 h, III: GR_36 h/GR_12 h) based on the RNA-seq analysis. Genes expressed at very low levels (RPKM < 10) in all conditions were not included. (B) Identification of the differentially expressed genes upon GR (GR_12 h/1%_12 h) in the glycolytic pathway. Enzymes shown in red and green color indicate upregulation and downregulation, respectively. GK, Glucokinase; GPI, Glucose phosphate isomerase; PFK, Phosphofructokinase; ALDO, Fructose-1,6-bisP aldolase; TPI, Triose-phosphate isomerase; GAPDH, glyceraldehyde 3-P dehydrogenase, PGK, Phosphoglycerate kinase; PGAM, phosphoglycerate mutase; ENO, Enolase; PEPCK, Phosphoenolpyruvate carboxykinase, MDH, Malate dehydrogenase; PK, Pyruvate kinase; ME, malic enzyme; ALT, Alanine aminotransferase; ADH, Alcohol dehydrogenase; LDH, Lactate dehydrogenase.

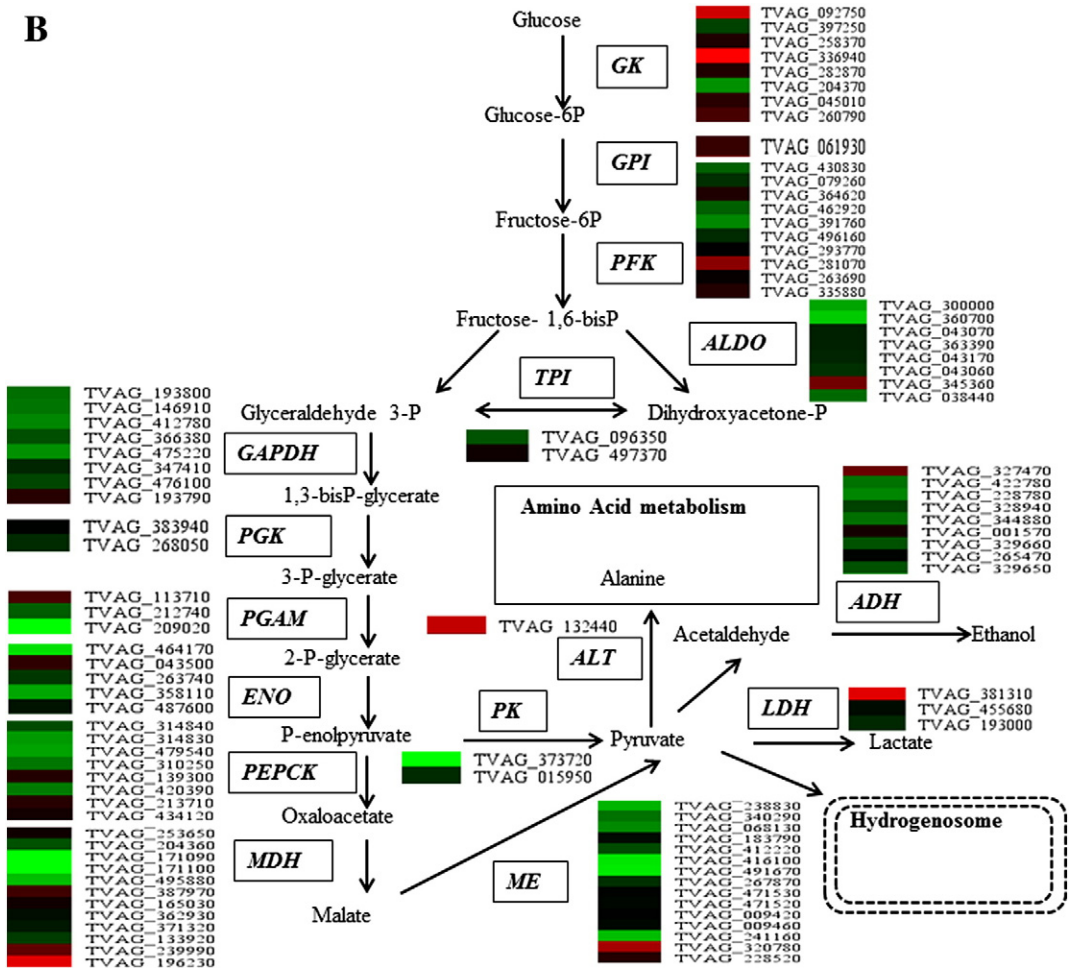

Fig. 3. (*continued*).

expression of genes involved in hydrogenosomal energy metabolism (Table S2). We noted that 6 of 7 genes encoding hydrogenosomal malic enzyme, which catalyzes the oxidative decarboxylation of malate to pyruate, were downregulated during GR (total RPKM for glucose-rich and GR_12 h were 22,512 and 6881, respectively). Suppression of this reaction in the hydrogenosome suggested that relatively low levels of pyruvate were generated through general energy metabolism under GR. Another line of evidence also indicated that pyruvate was preferentially metabolized to end products alanine or lactate due to overexpression of alanine aminotransferase (TVAG_132440) and lactate dehydrogenase (TVAG_381310) (Fig. 3B). Acetyl-CoA production catalyzed via pyruvate:ferredoxin oxidoreductase is utilized by the following two steps for ATP production. Particularly noteworthy is that the key enzymes Acetyl-CoA hydrolase gene family (TVAG_164890, TVAG_395550) (total RPKM for glucose-rich and GR_12 h were 1299 and 281, respectively) and succinate thiokinase (TVAG_183500, TVAG_144730, TVAG_259190, TVAG_047890, TVAG_318670) (total RPKM for glucose-rich and GR_12 h were 6916 and 5021, respectively), which catalyze ATP synthesis, were also downregulated at the log phase of GR, reaffirming that the hydrogenosomal energy metabolism was repressed in response to glucose deprivation.

3.4.2. Amino acid metabolism

Amino acids have been shown to sustain trichomonad growth and survival under carbohydrate-deficient conditions [57]. The arginine dihydrolase pathway has been considered to contribute to energy metabolism in *T. vaginalis* [58]. We found that two components involving the energy production of this pathway, ornithine carbamoyltransferase (TVAG_041310; no.13) (total RPKM for glucose-rich and GR_12 h were 1232 and 2395, respectively) and carbamate kinase (TVAG_261970; no.14), were upregulated in the log growth phase of GR-cultivated cells (Fig. 4A and Table S3), suggesting that this energy-producing pathway was important for cell division under GR. Methionine catabolism contains two degradation pathways, including the conversion of methionine to α-ketobutyrate or homocysteine. Two components involving the conversion of methionine to homocysteine, S-adenosylmethionine synthetase (TVAG_252200; no.32, the only paralogue with RPKM > 10 under glucose-rich condition) and adenosylhomocysteinase (TVAG_405240 and TVAG_210320; no.34), were significantly downregulated at the log phase of GR cultivation (Fig. 4B and Table S3). Downregulation of S-adenosylmethionine synthetase, which catalyzes the conversion of methionine to S-adenosylmethionine with ATP consumption, suggested that the energy-consuming reaction was suppressed during cell division under GR.

3.4.3. GR induces overexpression of aminotransferases

We noted an intriguing expression patterns of gene encoding enzymes involved in glutamate-related metabolic pathways that have not yet been characterized in *T. vaginalis* (Fig. 4C). Most of these enzymes are aminotransferases, which catalyze the transfer of amino group from a donor molecule to a recipient. There are 25

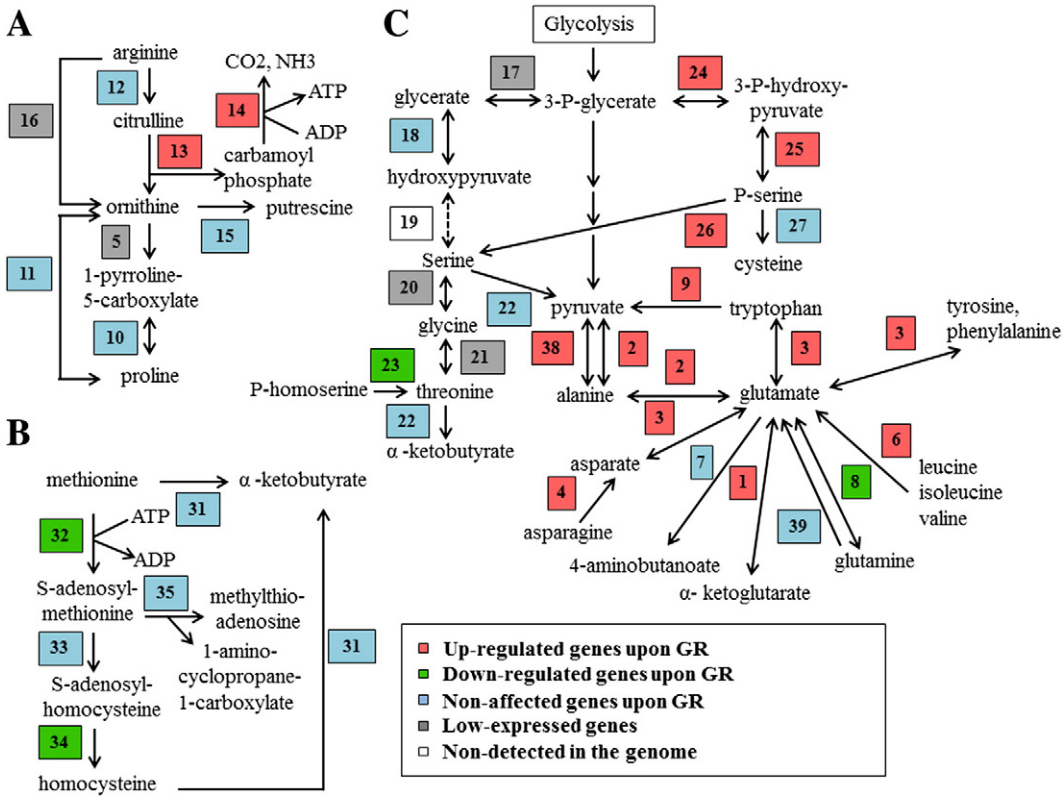

Fig. 4. The effects of GR on differential expression of genes encoding enzymes involved in amino acid metabolism of *T. vaginalis*. Differentially expressed genes determined by RNA-seq were mapped to known putative amino acid metabolic pathways in *T. vaginalis*, including the arginine dihydrolase pathway (A), methionine metabolism (B), and other amino acids metabolism (C). The numbers represented the enzymes catalyzing the reactions and their complete description was provided in Table S3. Enzymes shown in red and green rectangles indicate upregulation and downregulation at the log phase of GR (GR_12 h) compared with that of glucose-rich cultivation (1%_12 h), respectively, whereas those shown in blue and gray indicate the gene expression with no significant change or at very low levels (RPKM < 10). White rectangles represented enzymes that were not identified in the *T. vaginalis* genome.

aminotransferases identified in the *T. vaginalis* genome, representing 11 distinct groups [47]. Although a survey of aminotransferase activities in cell-free extract has been performed [59], the biological importance of these enzymes remains largely unknown. 7 groups of aminotransferase were upregulated at the log growth phase of GR cultivation, maintaining their high levels of expression at least for 36 h (Fig. 5A and Table S3). For instance, alanine aminotransferase (TVAG_132440, no.2) and alanine dehydrogenase (TVAG_235800 and TVAG_445130; no.38), which catalyze the reversible conversion of alanine to pyruvate or glutamate, increased expression more than 10-fold and 50-fold, respectively, at GR_12 h compared with glucose-rich cultivation. The expression of all aspartate aminotransferase paralogues (no.3) involved in the conversion of glutamate and other amino acid, such as aspartate, tyrosine, phenylalanine and typtophan, was also highly increased. Furthermore, the genes encoding branched-chain amino acid aminotransferase (TVAG_026740; TVAG_139240, no. 6), which mediated the conversion of leucine, isoleucine and valine to glutamate, were also significantly induced upon GR (total RPKM for glucose-rich and GR_12 h were 354 and 1930, respectively).

3.4.4. Glutamate dehydrogenase (GDH) was dramatically induced by GR

Among the aminotransferases, GDH represented the most upregulated genes during GR whose expression contributed to approximately 60% of total aminotransferases under GR (Fig. 5A and Table S3). GDH is a highly conserved enzyme catalyzing the reversible oxidative deamination of glutamate into α-ketoglutarate [60]. There are four GDH (TVAG_TVAG_025980; TVAG_025910; TVAG_072100; TVAG_201620) isoforms identified in the *T. vaginalis* genome [47]. GDH (TVAG_201620) was the major isoform expressed in the log phase under glucose-rich cultivation. It was highly induced and became the top 10 most expressed genes at the early stage of GR (before GR_36 h) (File S1). Other GDH isoforms, which express at very low levels (RPKM < 10) in the glucose-rich group, also represented the top 100 most expressed genes under GR before 36 h (File S1), suggesting that all GDH family genes were activated in response to GR. We validated the expression of GDH family genes by qPCR (Fig. S2). The quantitative data showed that GDHs were remarkably expressed during GR, especially at 36 h. We also evaluated the GDH activity during GR compared with glucose-rich condition, indicating that GR significantly increased the level of GDH activity, correlating with its expression levels (Fig. 5B).

GDH is a mitochondrial enzyme that regulates glutamate biogenesis and breakdown, linking the carbohydrate and protein metabolisms in the majority of eukaryotic cells. The enzyme is also of importance for ammonia detoxification and urea synthesis in the liver [61]. GDH activity is allosterically modulated by the energetic status of cells [60]. GDP and ADP positively regulate the GDH activity, whereas ATP and GTP suppress its activity. Hence, under caloric restriction (CR) or low glucose conditions, GDH is upregulated to produce α-ketoglutarate that can enter tricarboxylic acid (TCA) cycle directly for ATP generation [62]. Recently, GDH has been identified in the hydrogenosome proteome [48]. However, hydrogenosomes lack a TCA cycle; thus the upregulation of GDH in energy production may involve previously uncharacterized mechanisms. SIRT4, the mammalian homologues of sir2 that connects metabolism and longevity in several model organisms, has been shown to repress the GDH activity and oppose the effects of CR in pancreatic β cells [62]. GDH is abundantly expressed by *P. falciparum* and has been recognized as a

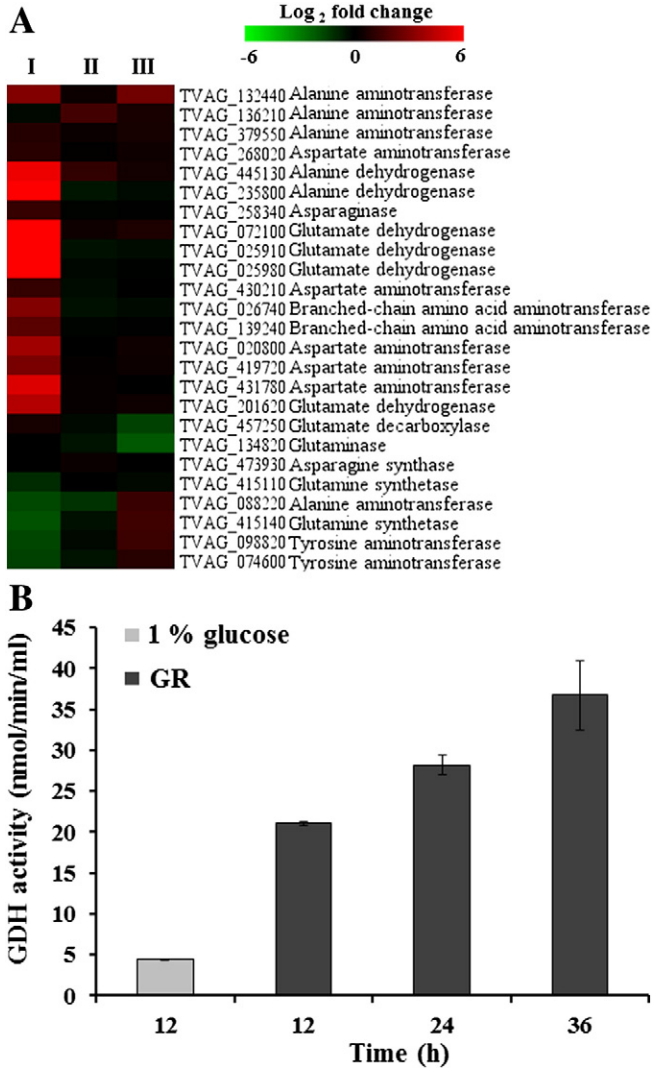

Fig. 5. GDH is overexpressed under GR in *T. vaginalis*. (A) Heatmap showing the gene expression patterns of aminotransferases at log phase of GR (GR_12 h) compared with that of glucose-rich (1%_12 h) cultivation and during stationary phase of GR (GR_24 h, GR_36 h) compared with log phase (GR_12 h). The gene expression changes were represented as $\log_2$ fold changes of RPKM (I: GR_12 h/1%_12 h, II: GR_24 h/GR_12 h, III: GR_36 h/GR_12 h) based on the RNA-seq analysis. The detailed gene expression profiles of aminotransferases were provided in Table S3. (B) Determination of GDH activity under 1% glucose and GR cultivation.

marker for malaria infection due to its absence from the host red blood cell. Therefore, GDH has been proposed as an antimalarial target [63]. The deamination reaction catalyzed by GDH produces ammonia, which plays a crucial role in acid/base balance. Hence, another possible role of GDH in this parasite may be the regulator of pH homeostasis upon GR. We highlighted the potentially important roles of GDH in *T. vaginalis* during GR; however, more efforts are needed to elucidate the complex regulatory networks of the aminotransferase in this parasite.

3.5. Modulation of autophagy in T. vaginalis

3.5.1. Identification of autophagic machinery in T. vaginalis

Autophagy is considered a cytoprotective mechanism that allows cells to degrade their cytosolic components for survival under nutrient deprivation. Hydrogenosome autophagy has been identified in *Tritrichomonas foetus* by ultrastructural analyses using electron microscopy [64]. However, very little is known about the autophagic process at the molecular level in trichomonads. To further characterize the molecular components of autophagy in *T. vaginalis*, BLAST searches for Atg orthologues in the genome were performed (Table S4). We identified a total of 27 putative Atg sequences in *T. vaginalis*, representing 10 distinct *Atg* genes with sequence similarity to those in yeast and mammals. Our data, in consistence with previous genome-wide analyses for Atg orthologues in *T. vaginalis* [65,66], indicated that the parasite encodes a limited repertoire of putative Atg proteins. Additionally, Atg4 and Atg8, key molecules involved in autophagosome biosynthesis, were characterized by more than one paralogue. Atg8 requires the activity of two conjugation systems, Atg5-to-Atg12 and Atg4-Atg7-Atg3, to bind to the autophagosomal membrane. Of note, *T. vaginalis* only possesses Atg8-Atg4-Atg7-Atg3 conjugation system but lacks Atg5-to-Atg12, suggesting the different autophagy pathway from yeast and mammals. Similar results have been reported in other protists, including Leishmania [67], Dictyostelium [68], Entamoeba [21] and *T. gondii* [69], implying that Atg8 conjugation system may be evolutionarily older and possibly the minimal machinery required for autophagosome formation. Atg8 has been widely used as a specific marker for autophagosome detection. Amino acid sequences of Atg8 from different organisms were aligned (Fig. S3A), indicating a conserved functional domain of Atg8 in *T. vaginalis* (TVAG_486080, TvAtg8a; TVAG_239800, TvAtg8b) (Fig. S3C). Additionally, TvAtg8 showed sequence identities less than 50% with other protozoan (Fig. S3B), suggesting a unique feature of Atg8 in this parasite. Hence, further characterization of the Atg8-associated core machinery in *T. vaginalis* will reveal a distinct autophagy regulatory network in the deep-branching protozoan. Based on the RNA-seq data, we noticed that Atg4 (TVAG_023970) and Atg8 (TVAG_486080) represented the most abundant transcript among their multiple paralogues and their expression levels appeared to be upregulated upon GR (Table S5); however, further investigations are needed to clarify the functions of these putative Atg orthologues in this parasite.

3.5.2. GR induces autophagy in T. vaginalis

To assess whether GR is able to induce autophagy in *T. vaginalis*, cells cultivated under GR at different time intervals (12 h, 24 h, 36 h) and glucose-rich medium (1% glucose-12 h) were harvested and stained with Cyto-ID™, a fluorescent autophagy tracker for the rapid detection of autophagic vacuoles in live cells [32,33,70] (Fig. 6A). This probe is a cationic amphiphilic tracer dye that has been optimized through the identification of titratable functional moieties, allowing for minimal staining of lysosomes while exhibiting bright fluorescence upon incorporation into autophagosomes and autolysosomes. The data showed that almost no autophagosome-like vacuole was detected in cells in the log phases of glucose-rich and GR cultivation (GR_12 h), suggesting that autophagy was not triggered under glucose-rich condition. Conversely, autophagosome-like vesicles were significantly increased under GR after 24 h and were maintained at a higher level for at least 36 h. Quantification of autophagic signals by flow cytometric analysis indicated that the punctuate signals were indeed highly induced from GR_24 h (Fig. 6A). Hence, we demonstrated for the first time that GR induces autophagy-like response in *T. vaginalis*. To evaluate that the punctuate structures were indeed autophagosomes, cells cultivated under GR were treated with the most commonly used autophagy inhibitor wortmannin and monitored the vesicles by the same approach. Wortmannin is a well-known fungal phosphatidylinositol (PI) 3-kinase inhibitor that suppresses the formation of autophagosome in yeast [71], as well as in several protists, such as *E. histolytica* [21], *Blastocystis* [22], and *T. brucei* [23]. Consistent with the previous observations, autophagic vesicles were highly reduced in GR-cultured cells after treatment with wortmannin for 6 h (the average number of punctate per cell for GR_24 h and GR_36_h cells decreased from 11.9 ± 0.3 and 12.5 ± 2.7 to 5.3 ± 1 and 3 ± 1.3, respectively) (Fig. 6B). Thus,

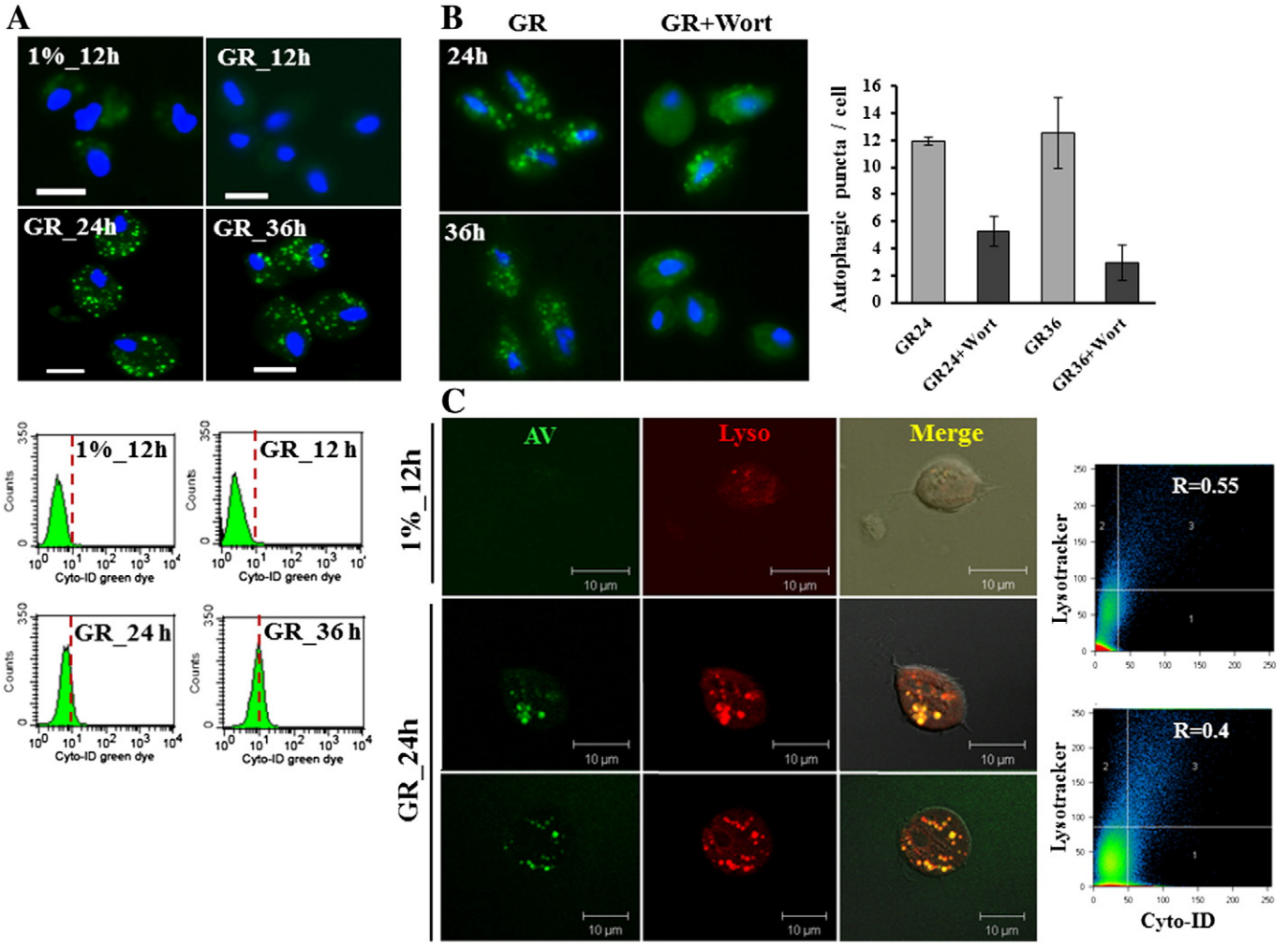

Fig. 6. GR induces autophagy in *T. vaginalis*. (A) Fluorescent images of autophagy detection in cells cultivated under glucose-rich (1% glucose) and GR conditions were shown. The mid-log phase of glucose-rich (1%_12 h) and GR-cultivated cells (GR_12 h) and the stationary phase of GR-cultivated cells at different time intervals (24 h, 36 h) were stained with Cyto-ID™ autophagic green fluorescent dye for 30 min at 37 °C and viewed under a fluorescent microscopy. Quantitative fluorescent signals were determined by FASCan flow cytometer. Scale bars = 10 μm. (B) Inhibition of autophagy by wortmannin in *T. vaginalis*. GR-cultured cells at different time intervals (24 h, 36 h) were treated with 50 μM wortmannin (wort) for 6 h. The cells were stained with autophagic green fluorescent dye for 30 min at 37 °C and viewed under a fluorescent microscopy. The average number of autophagic vesicles per cell was determined by manual calculation after treatment with wort compared to the untreated groups. Data represented the means ± SD of two groups (40 cells per group) for each condition. (C) Co-localization of autophagosomes with lysosomes. Approximately 3×10^5 cells from the glucose-rich cultivation (1%_12 h) and GR_24 h were harvested and co-stained with autophagic green fluorescent dye (AV) and lysosome indicator Lysotracker Red (Lyso) for 30 min at 37 °C, and then analyzed by using a confocal microscope. Co-localization diagrams of the two representative cells (GR_24 h) showing the fluorescent intensity of the fluorophores (x axis = Cyto-ID™ green dye; y axis = Lysotracker Red) and their co-localization correlation determined by Pearson's correlation coefficient (R).

the data suggested a similar regulation pathway for autophagy inhibition in *T. vaginalis*.

To evaluate whether the lysosomal-mediated degradation process exists in *T. vaginalis* during GR, we detected the co-localization of autophagic punctuate with Lysotracker Red, a widely used marker for staining lysosomes [22]. The data indicated that autophagosome-like vacuoles induced by GR at 24 h remarkably co-localized with lysosomes (the mean value of the Pearson's correlation coefficient was 0.5 ± 0.07, n = 11), whereas almost no co-localization signals were observed at the log phase of glucose-rich cultivation (Fig. 6C). This observation confirmed the nature of autophagy that autophagosomes fuse with lysosomes in *T. vaginalis*. Based on the research platforms established, it is feasible to investigate the mechanistic details of this biologically significant and distinct process in trichomonads, paving the way for characterization of evolution of autophagy in different organisms and possibly for the development of new therapeutics against trichomoniasis.

4. Conclusions

Altogether, we demonstrated that *T. vaginalis* possesses several adaptive mechanisms elicited by GR, including enhancement of cell survival, antioxidant ability, and autophagy. On the basis of these findings, we proposed a model depicting the possible strategies used by *T. vaginalis* to establish an infection in the vagina (Fig. 7). This is the first report providing an in-depth analysis of the transcriptomic signatures under standard glucose-rich and GR cultivation using RNA-seq, highlighting genes potentially involved in the adaptive responses to GR. The highly-induced genes during the metabolic stress may play pivotal roles for *T. vaginalis* to establish an infection, and thereby may be potential drug targets against infection of this common but neglected human pathogen.

Supplementary data to this article can be found online at http://dx.doi.org/10.1016/j.bbagen.2013.08.008.

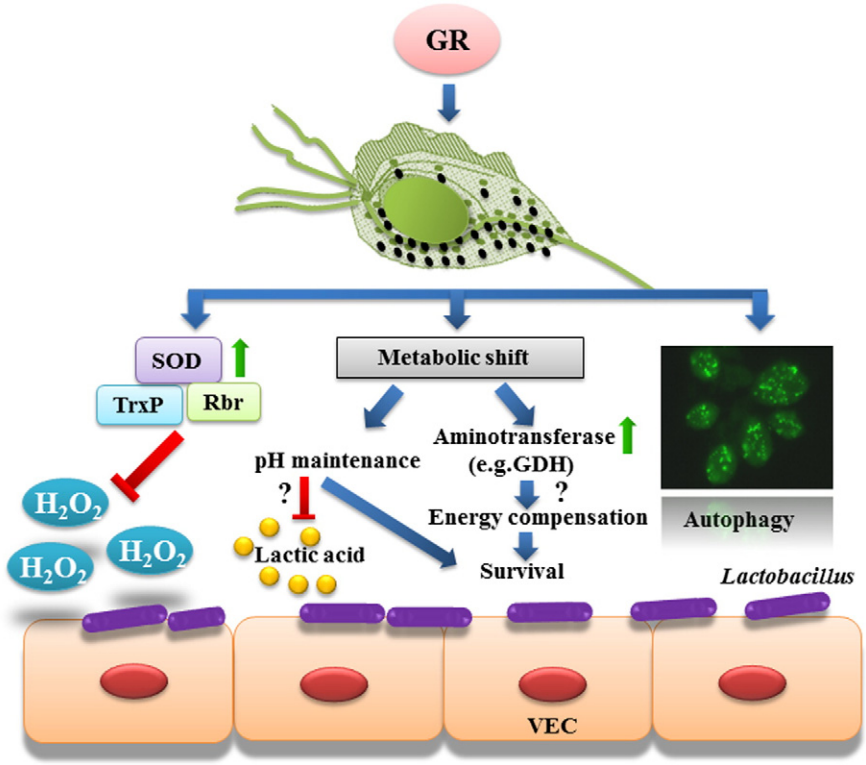

Fig. 7. A proposed model for adaptive responses of *T. vaginalis* to GR. Antioxidant genes, such as SOD, TrxP, and Rbr, were upregulated in response to GR, possibly enhancing the anti-H_2O_2 capability of *T. vaginalis*. Additionally, metabolism through GR revealed metabolic shift that maintained the pH suitable for survival. Moreover, GR elicited upregulation of aminotransferase, such as GDH, which is a proposed mechanism for energetic compensation under nutritional stress. Finally, autophagy, the process responsible for starvation, was triggered upon GR in *T. vaginalis*. VEC, vaginal epithelial cells.

Acknowledgements

This work was supported by the Chang Gung Memorial Hospital Research Funding (CMRPD1B0441-3) and National Science Council, Taiwan (NSC-101-2320-B182-025-MY3) to PT.

References

[1] A.C. Ferretti, M.C. Larocca, C. Favre, Nutritional stress in eukaryotic cells: oxidative species and regulation of survival in time of scarceness, Mol. Genet. Metab. 105 (2011) 186–192.
[2] L. Fontana, L. Partridge, V.D. Longo, Extending healthy life span—from yeast to humans, Science 328 (2010) 321–326.
[3] C.R. Burtner, C.J. Murakami, B.K. Kennedy, M. Kaeberlein, A molecular mechanism of chronological aging in yeast, Cell Cycle 8 (2009) 1256–1270.
[4] M. Kaeberlein, R.W. Powers III, K.K. Steffen, E.A. Westman, D. Hu, N. Dang, E.O. Kerr, K.T. Kirkland, S. Fields, B.K. Kennedy, Regulation of yeast replicative life span by TOR and Sch9 in response to nutrients, Science 310 (2005) 1193–1196.
[5] P. Fabrizio, V.D. Longo, The chronological life span of *Saccharomyces cerevisiae*, Methods Mol. Biol. 371 (2007) 89–95.
[6] Y. Inoue, D.J. Klionsky, Regulation of macroautophagy in *Saccharomyces cerevisiae*, Semin. Cell Dev. Biol. 21 (2010) 664–670.
[7] M.M. Hobbs, A.C. Sena, H. Swygard, J.R. Schwebke, *Trichomonas vaginalis* and trichomoniasis, in: K.K. Holmes, P.F. Sparling, W.E. Stamm, et al., (Eds.), Sexually Transmitted Diseases, McGraw-Hill Medical, New York, 2008, pp. 771–793.
[8] W.A. Gardner Jr., D.E. Culberson, B.D. Bennett, *Trichomonas vaginalis* in the prostate gland, Arch. Pathol. Lab. Med. 110 (1986) 430–432.
[9] R.S. McClelland, L. Sangare, W.M. Hassan, L. Lavreys, K. Mandaliya, J. Kiarie, J. Ndinya-Achola, W. Jaoko, J.M. Baeten, Infection with *Trichomonas vaginalis* increases the risk of HIV-1 acquisition, J. Infect. Dis. 195 (2007) 698–702.
[10] S. Sutcliffe, J.F. Alderete, C. Till, P.J. Goodman, A.W. Hsing, J.M. Zenilman, A.M. De Marzo, E.A. Platz, Trichomonosis and subsequent risk of prostate cancer in the Prostate Cancer Prevention Trial, Int. J. Cancer 124 (2009) 2082–2087.
[11] M. Muller, Energy metabolism of protozoa without mitochondria, Annu. Rev. Microbiol. 42 (1988) 465–488.
[12] A. Steinbuchel, M. Muller, Anaerobic pyruvate metabolism of *Tritrichomonas foetus* and *Trichomonas vaginalis* hydrogenosomes, Mol. Biochem. Parasitol. 20 (1986) 57–65.
[13] J. Fang, H. Zhou, D. Rathore, M. Sullivan, X.Z. Su, T.F. McCutchan, Ambient glucose concentration and gene expression in *Plasmodium falciparum*, Mol. Biochem. Parasitol. 133 (2004) 125–129.
[14] D. Eichinger, A role for a galactose lectin and its ligands during encystment of Entamoeba, J. Eukaryot. Microbiol. 48 (2001) 17–21.
[15] A. Tovy, R. Hertz, R. Siman-Tov, S. Syan, D. Faust, N. Guillen, S. Ankri, Glucose starvation boosts *Entamoeba histolytica* virulence, PLoS Negl. Trop. Dis. 5 (2011) e1247.
[16] S. Baumel-Alterzon, C. Weber, N. Guillen, S. Ankri, Identification of dihydropyrimidine dehydrogenase as a virulence factor essential for the survival of *Entamoeba histolytica* in glucose-poor environments, Cell. Microbiol. 15 (2013) 130–144.
[17] L.S. Diamond, C.G. Clark, C.C. Cunnick, YI-S, a casein-free medium for axenic cultivation of Entamoeba histolytica, related Entamoeba, *Giardia intestinalis* and *Trichomonas vaginalis*, J. Eukaryot. Microbiol. 42 (1995) 277–278.
[18] M. Duszenko, M.L. Ginger, A. Brennand, M. Gualdron-Lopez, M.I. Colombo, G.H. Coombs, I. Coppens, B. Jayabalasingham, G. Langsley, S.L. de Castro, R. Menna-Barreto, J.C. Mottram, M. Navarro, D.J. Rigden, P.S. Romano, V. Stoka, B. Turk, P.A. Michels, Autophagy in protists, Autophagy 7 (2011) 127–158.
[19] S. Besteiro, R.A.M. Williams, L.S. Morrison, G.H. Coombs, J.C. Mottram, Endosome sorting and autophagy are essential for differentiation and virulence of Leishmania major, J. Biol. Chem. 281 (2006) 11384–11396.
[20] V.E. Alvarez, G. Kosec, C.S. Anna, V. Turk, J.J. Cazzulo, B. Turk, Autophagy is involved in nutritional stress response and differentiation in *Trypanosoma cruzi*, J. Biol. Chem. 283 (2008) 3454–3464.
[21] K. Picazarri, K. Nakada-Tsukui, T. Nozaki, Autophagy during proliferation and encystation in the protozoan parasite *Entamoeba invadens*, Infect. Immun. 76 (2008) 278–288.
[22] J. Yin, A.J.J. Ye, K.S.W. Tan, Autophagy is involved in starvation response and cell death in Blastocystis, Microbiology 156 (2010) 665–677.
[23] F.J. Li, Q. Shen, C. Wang, Y. Sun, A.Y. Yuan, C.Y. He, A role of autophagy in *Trypanosoma brucei* cell death, Cell. Microbiol. 14 (2012) 1242–1256.
[24] D. Ghosh, J.L. Walton, P.D. Roepe, A.P. Sinai, Autophagy is a cell death mechanism in *Toxoplasma gondii*, Cell. Microbiol. 14 (2012) 589–607.
[25] S.C. Schuster, Next-generation sequencing transforms today's biology, Nat. Methods 5 (2008) 16–18.
[26] W.C. Lin, K.Y. Huang, S.C. Chen, T.Y. Huang, S.J. Chen, P.J. Huang, P. Tang, Malate dehydrogenase is negatively regulated by miR-1 in *Trichomonas vaginalis*, Parasitol. Res. 105 (2009) 1683–1689.
[27] R.A. Barrero, B. Chapman, Y. Yang, P. Moolhuijzen, G. Keeble-Gagnere, N. Zhang, Q. Tang, M.I. Bellgard, D. Qiu, De novo assembly of *Euphorbia fischeriana* root transcriptome identifies prostratin pathway related genes, BMC Genomics 12 (2011) 600.

[28] C. Aurrecoechea, J. Brestelli, B.P. Brunk, J.M. Carlton, J. Dommer, S. Fischer, B. Gajria, X. Gao, A. Gingle, G. Grant, O.S. Harb, M. Heiges, F. Innamorato, J. Iodice, J.C. Kissinger, E. Kraemer, W. Li, J.A. Miller, H.G. Morrison, V. Nayak, C. Pennington, D.F. Pinney, D.S. Roos, C. Ross, C.J. Stoeckert Jr., S. Sullivan, C. Treatman, H. Wang, GiardiaDB and TrichDB: integrated genomic resources for the eukaryotic protist pathogens *Giardia lamblia* and *Trichomonas vaginalis*, Nucleic Acids Res. 37 (2009) D526–D530.
[29] K. Homma, K. Suzuki, H. Sugawara, The Autophagy Database: an all-inclusive information resource on autophagy that provides nourishment for research, Nucleic Acids Res. 39 (2011) D986–D990.
[30] S.F. Altschul, T.L. Madden, A.A. Schaffer, J. Zhang, Z. Zhang, W. Miller, D.J. Lipman, Gapped BLAST and PSI-BLAST: a new generation of protein database search programs, Nucleic Acids Res. 25 (1997) 3389–3402.
[31] A. Marchler-Bauer, S. Lu, J.B. Anderson, F. Chitsaz, M.K. Derbyshire, C. DeWeese-Scott, J.H. Fong, L.Y. Geer, R.C. Geer, N.R. Gonzales, M. Gwadz, D.I. Hurwitz, J.D. Jackson, Z. Ke, C.J. Lanczycki, F. Lu, G.H. Marchler, M. Mullokandov, M.V. Omelchenko, C.L. Robertson, J.S. Song, N. Thanki, R.A. Yamashita, D. Zhang, N. Zhang, C. Zheng, S.H. Bryant, CDD: a Conserved Domain Database for the functional annotation of proteins, Nucleic Acids Res. 39 (2011) D225–D229.
[32] H.M. Warenius, J.D. Kilburn, J.W. Essex, R.I. Maurer, J.P. Blaydes, U. Agarwala, L.A. Seabra, Selective anticancer activity of a hexapeptide with sequence homology to a non-kinase domain of Cyclin Dependent Kinase 4, Mol. Cancer 10 (2011) 72.
[33] A.K. Klappan, S. Hones, I. Mylonas, A. Bruning, Proteasome inhibition by quercetin triggers macroautophagy and blocks mTOR activity, Histochem. Cell Biol. 137 (2012) 25–36.
[34] T. Tra, L. Gong, L.P. Kao, X.L. Li, C. Grandela, R.J. Devenish, E. Wolvetang, M. Prescott, Autophagy in human embryonic stem cells, PLoS One 6 (2011) e27485.
[35] J. Adler, I. Parmryd, Quantifying colocalization by correlation: the Pearson correlation coefficient is superior to the Mander's overlap coefficient, Cytometry A 77 (2010) 733–742.
[36] K.Y. Huang, P.J. Huang, F.M. Ku, R. Lin, J.F. Alderete, P. Tang, Comparative transcriptomic and proteomic analyses of *Trichomonas vaginalis* following adherence to fibronectin, Infect. Immun. 80 (2012) 3900–3911.
[37] S. Ehrstrom, A. Yu, E. Rylander, Glucose in vaginal secretions before and after oral glucose tolerance testing in women with and without recurrent vulvovaginal candidiasis, Obstet. Gynecol. 108 (2006) 1432–1437.
[38] A. Surexh, A. Rajesh, R. Bhat, M.Y. Rai, Cytolytic vaginosis: a review, Indian J. Sex Transm. Dis. 30 (2009) 48–50.
[39] B.K. Kennedy, K.K. Steffen, M. Kaeberlein, Ruminations on dietary restriction and aging, Cell. Mol. Life Sci. 64 (2007) 1323–1328.
[40] M. Kaeberlein, Lessons on longevity from budding yeast, Nature 464 (2010) 513–519.
[41] S.L. Cudmore, K.L. Delgaty, S.F. Hayward-McClelland, D.P. Petrin, G.E. Garber, Treatment of infections caused by metronidazole-resistant *Trichomonas vaginalis*, Clin. Microbiol. Rev. 17 (2004) 783–793(table of contents).
[42] L. Horvathova, L. Safarikova, M. Basler, I. Hrdy, N.B. Campo, J.W. Shin, K.Y. Huang, P.J. Huang, R. Lin, P. Tang, J. Tachezy, Transcriptomic Identification of iron-regulated and iron-independent gene copies within the heavily duplicated *Trichomonas vaginalis* genome, Genome Biol. Evol. 4 (2012) 905–917.
[43] S.E. Babbitt, L. Altenhofen, S.A. Cobbold, E.S. Istvan, C. Fennell, C. Doerig, M. Llinas, D.E. Goldberg, *Plasmodium falciparum* responds to amino acid starvation by entering into a hibernatory state, Proc. Natl. Acad. Sci. U. S. A. 109 (2012) E3278–E3287.
[44] A. Mesquita, M. Weinberger, A. Silva, B. Sampaio-Marques, B. Almeida, C. Leao, V. Costa, F. Rodrigues, W.C. Burhans, P. Ludovico, Caloric restriction or catalase inactivation extends yeast chronological lifespan by inducing H2O2 and superoxide dismutase activity, Proc. Natl. Acad. Sci. U. S. A. 107 (2010) 15123–15128.
[45] T.J. Schulz, K. Zarse, A. Voigt, N. Urban, M. Birringer, M. Ristow, Glucose restriction extends *Caenorhabditis elegans* life span by inducing mitochondrial respiration and increasing oxidative stress, Cell Metab. 6 (2007) 280–293.
[46] A.A. Petti, C.A. Crutchfield, J.D. Rabinowitz, D. Botstein, Survival of starving yeast is correlated with oxidative stress response and nonrespiratory mitochondrial function, Proc. Natl. Acad. Sci. U. S. A. 108 (2011) E1089–E1098.
[47] J.M. Carlton, R.P. Hirt, J.C. Silva, A.L. Delcher, M. Schatz, Q. Zhao, J.R. Wortman, S.L. Bidwell, U.C. Alsmark, S. Besteiro, T. Sicheritz-Ponten, C.J. Noel, J.B. Dacks, P.G. Foster, C. Simillion, Y. Van de Peer, D. Miranda-Saavedra, G.J. Barton, G.D. Westrop, S. Muller, D. Dessi, P.L. Fiori, Q. Ren, I. Paulsen, H. Zhang, F.D. Bastida-Corcuera, A. Simoes-Barbosa, M.T. Brown, R.D. Hayes, M. Mukherjee, C.Y. Okumura, R. Schneider, A.J. Smith, S. Vanacova, M. Villalvazo, B.J. Haas, M. Pertea, T.V. Feldblyum, T.R. Utterback, C.L. Shu, K. Osoegawa, P.J. de Jong, I. Hrdy, L. Horvathova, Z. Zubacova, P. Dolezal, S.B. Malik, J.M. Logsdon Jr., K. Henze, A. Gupta, C.C. Wang, R.L. Dunne, J.A. Upcroft, P. Upcroft, O. White, S.L. Salzberg, P. Tang, C.H. Chiu, Y.S. Lee, T.M. Embley, G.H. Coombs, J.C. Mottram, J. Tachezy, C.M. Fraser-Liggett, P.J. Johnson, Draft genome sequence of the sexually transmitted pathogen *Trichomonas vaginalis*, Science 315 (2007) 207–212.
[48] R.E. Schneider, M.T. Brown, A.M. Shiflett, S.D. Dyall, R.D. Hayes, Y. Xie, J.A. Loo, P.J. Johnson, The *Trichomonas vaginalis* hydrogenosome proteome is highly reduced relative to mitochondria, yet complex compared with mitosomes, Int. J. Parasitol. 41 (2011) 1421–1434.
[49] G.H. Coombs, G.D. Westrop, P. Suchan, G. Puzova, R.P. Hirt, T.M. Embley, J.C. Mottram, S. Muller, The amitochondriate eukaryote *Trichomonas vaginalis* contains a divergent thioredoxin-linked peroxiredoxin antioxidant system, J. Biol. Chem. 279 (2004) 5249–5256.
[50] J.R. Cypser, T.E. Johnson, Multiple stressors in *Caenorhabditis elegans* induce stress hormesis and extended longevity, J. Gerontol. A Biol. Sci. Med. Sci. 57 (2002) B109–B114.
[51] E.J. Masoro, The role of hormesis in life extension by dietary restriction, Interdiscip. Top. Gerontol. 35 (2007) 1–17.
[52] B.P. Yu, H.Y. Chung, Stress resistance by caloric restriction for longevity, Ann. N. Y. Acad. Sci. 928 (2001) 39–47.
[53] N. Fitzsimmons, D.R. Berry, Inhibition of *Candida albicans* by Lactobacillus acidophilus: evidence for the involvement of a peroxidase system, Microbios 80 (1994) 125–133.
[54] D.C. St Amant, I.E. Valentin-Bon, A.E. Jerse, Inhibition of *Neisseria gonorrhoeae* by *Lactobacillus* species that are commonly isolated from the female genital tract, Infect. Immun. 70 (2002) 7169–7171.
[55] A. Lama, A. Kucknoor, V. Mundodi, J.F. Alderete, Glyceraldehyde-3-phosphate dehydrogenase is a surface-associated, fibronectin-binding protein of *Trichomonas vaginalis*, Infect. Immun. 77 (2009) 2703–2711.
[56] V. Mundodi, A.S. Kucknoor, J.F. Alderete, Immunogenic and plasminogen-binding surface-associated alpha-enolase of *Trichomonas vaginalis*, Infect. Immun. 76 (2008) 523–531.
[57] S.S. Pao, I.T. Paulsen, M.H. Saier Jr., Major facilitator superfamily, Microbiol. Mol. Biol. Rev. 62 (1998) 1–34.
[58] N. Yarlett, M.P. Martinez, M.A. Moharrami, J. Tachezy, The contribution of the arginine dihydrolase pathway to energy metabolism by *Trichomonas vaginalis*, Mol. Biochem. Parasitol. 78 (1996) 117–125.
[59] P.N. Lowe, A.F. Rowe, Aminotransferase activities in *Trichomonas vaginalis*, Mol. Biochem. Parasitol. 21 (1986) 65–74.
[60] M. Karaca, F. Frigerio, P. Maechler, From pancreatic islets to central nervous system, the importance of glutamate dehydrogenase for the control of energy homeostasis, Neurochem. Int. 59 (2011) 510–517.
[61] I. Nissim, Newer aspects of glutamine/glutamate metabolism: the role of acute pH changes, Am. J. Physiol. 277 (1999) F493–F497.
[62] M.C. Haigis, R. Mostoslavsky, K.M. Haigis, K. Fahie, D.C. Christodoulou, A.J. Murphy, D.M. Valenzuela, G.D. Yancopoulos, M. Karow, G. Blander, C. Wolberger, T.A. Prolla, R. Weindruch, F.W. Alt, L. Guarente, SIRT4 inhibits glutamate dehydrogenase and opposes the effects of calorie restriction in pancreatic beta cells, Cell 126 (2006) 941–954.
[63] I.M. Aparicio, A. Marin-Menendez, A. Bell, P.C. Engel, Susceptibility of *Plasmodium falciparum* to glutamate dehydrogenase inhibitors—a possible new antimalarial target, Mol. Biochem. Parasitol. 172 (2010) 152–155.
[64] M. Benchimol, Hydrogenosome autophagy: an ultrastructural and cytochemical study, Biol. Cell 91 (1999) 165–174.
[65] A. Brennand, M. Gualdron-Lopez, I. Coppens, D.J. Rigden, M.L. Ginger, P.A. Michels, Autophagy in parasitic protists: unique features and drug targets, Mol. Biochem. Parasitol. 177 (2011) 83–99.
[66] J.M. Carlton, S.B. Malik, S.A. Sullivan, T. Sicheritz-Ponten, P. Tang, R.P. Hirt, The genome of *Trichomonas vaginalis*, Anaerobic Parasitic Protozoa: Genomics and Molecular Biology, 2010, pp. 45–80.
[67] R.A. Williams, L. Tetley, J.C. Mottram, G.H. Coombs, Cysteine peptidases CPA and CPB are vital for autophagy and differentiation in *Leishmania mexicana*, Mol. Microbiol. 61 (2006) 655–674.
[68] G.P. Otto, M.Y. Wu, N. Kazgan, O.R. Anderson, R.H. Kessin, Macroautophagy is required for multicellular development of the social amoeba *Dictyostelium discoideum*, J. Biol. Chem. 278 (2003) 17636–17645.
[69] S. Besteiro, C.F. Brooks, B. Striepen, J.F. Dubremetz, Autophagy protein Atg3 is essential for maintaining mitochondrial integrity and for normal intracellular development of *Toxoplasma gondii* tachyzoites, PLoS Pathog. 7 (2011) e1002416.
[70] L.L. Chan, D. Shen, A.R. Wilkinson, W. Patton, N. Lai, E. Chan, D. Kuksin, B. Lin, J. Qiu, A novel image-based cytometry method for autophagy detection in living cells, Autophagy 8 (2012) 1371–1382.
[71] D.B. Munafo, M.I. Colombo, A novel assay to study autophagy: regulation of autophagosome vacuole size by amino acid deprivation, J. Cell Sci. 114 (2001) 3619–3629.